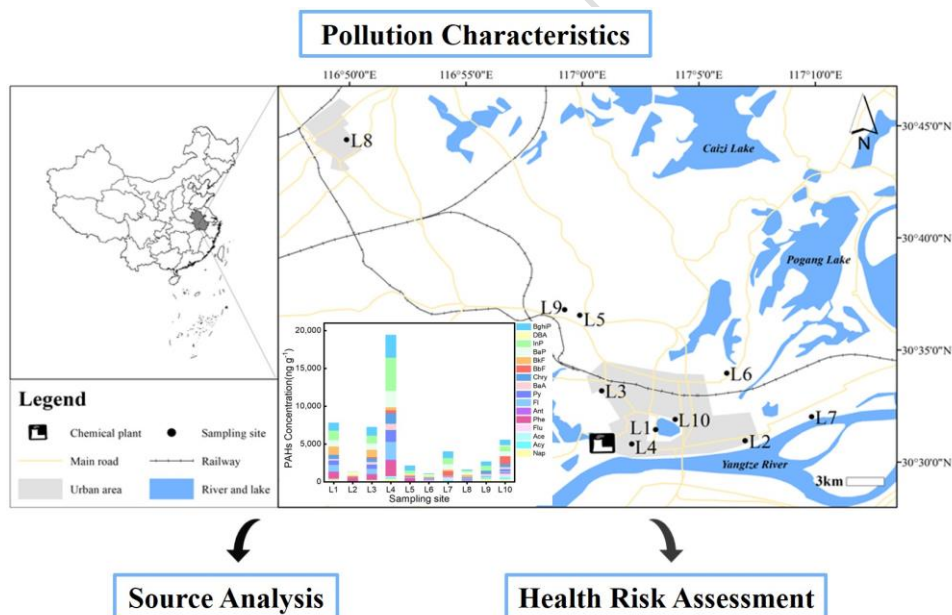


1 **Polycyclic aromatic hydrocarbons in atmospheric dust deposition**  
2 **from Anqing, China: pollution characteristics, sources and health risk**  
3 **assessment**

4 **Tian Yangji, Liu Ting, Li Fasong\*, Mei Xuan, Shi Jie, Fang Mengjun, Xu Bowen, Qiu**  
5 **Jianfeng**

6 College of Resources and Environment, Anqing Normal University, Anqing, Anhui 246011, China  
7 \*e-mail: lifs628@163.com;  
8 Tel.: +86-556-5306208.

9  
10 **Graphical abstract**



11  
12 **Source Analysis**

13 **Health Risk Assessment**

14  
15  
16  
17 **Abstract**

18 This study systematically analyzed the pollution characteristics, source apportionment, and health  
19 risks of 16 polycyclic aromatic hydrocarbons (PAHs) in atmospheric dust deposition, using Anqing  
20 City—a typical industrial city in China—as the research subject. Results indicate that the  
21 concentration range of  $\Sigma_{16}$ PAHs in atmospheric dust in Anqing City is 85.22–21,351.03 ng g<sup>-1</sup>, with

18 an average of 5,301.21 ng g<sup>-1</sup>, placing the pollution level in the lower-middle range nationally. Spatial  
19 distribution revealed significantly higher PAH concentrations in industrial clusters of Daguan District  
20 compared to other areas, indicating industrial emissions as a major point source of PAHs. The  
21 composition was dominated by high-ring (5–6 ring) PAHs (average proportion: 58.90%), indicating  
22 primary origin from high-temperature combustion processes. Integrated source apportionment using  
23 ring number distribution, characteristic ratio analysis, and positive matrix factorization (PMF) models  
24 identified fossil fuel combustion and industrial activities as the primary PAH sources. Health risk  
25 assessments revealed skin contact as the predominant exposure pathway for both adults and children,  
26 with carcinogenic risks approaching or exceeding acceptable thresholds under certain high-exposure  
27 scenarios.

28 **Keywords:** Polycyclic aromatic hydrocarbons; Atmospheric dust deposition; Health risk assessment;  
29 Anqing

30

### 31 1. Introduction

32 The presence of environmental pollutants represents a significant threat to human health. Among  
33 these pollutants, polycyclic aromatic hydrocarbons (PAHs) are of significant concern due to their  
34 toxicity, carcinogenicity, and teratogenicity(Barbosa Jr et al., 2023). PAHs constitute a diverse group  
35 of organic compounds found extensively in environmental matrices like road dust, soil, and  
36 sediments(Ma et al., 2017). In light of the pervasive presence of these compounds in the environment  
37 and their potential implications for human and ecological health, the United States Environmental  
38 Protection Agency (USEPA) has identified 16 PAHs as priority pollutants(Samburova et al., 2017).

39 Globally, a significant quantity of PAHs are released into the atmosphere on an annual basis, and  
40 since PAHs are mostly products of incomplete combustion, most of them primarily manifest as  
41 particulate matter, which will migrate and diffuse with the atmosphere, and finally land on the ground  
42 in the form of dust(Yang et al., 2021). In addition to direct harm to the human body, atmospheric dust

43 fall pollution will also produce some damage to humans and the environment through various  
44 environmental media(Kothiyal et al., 2022).

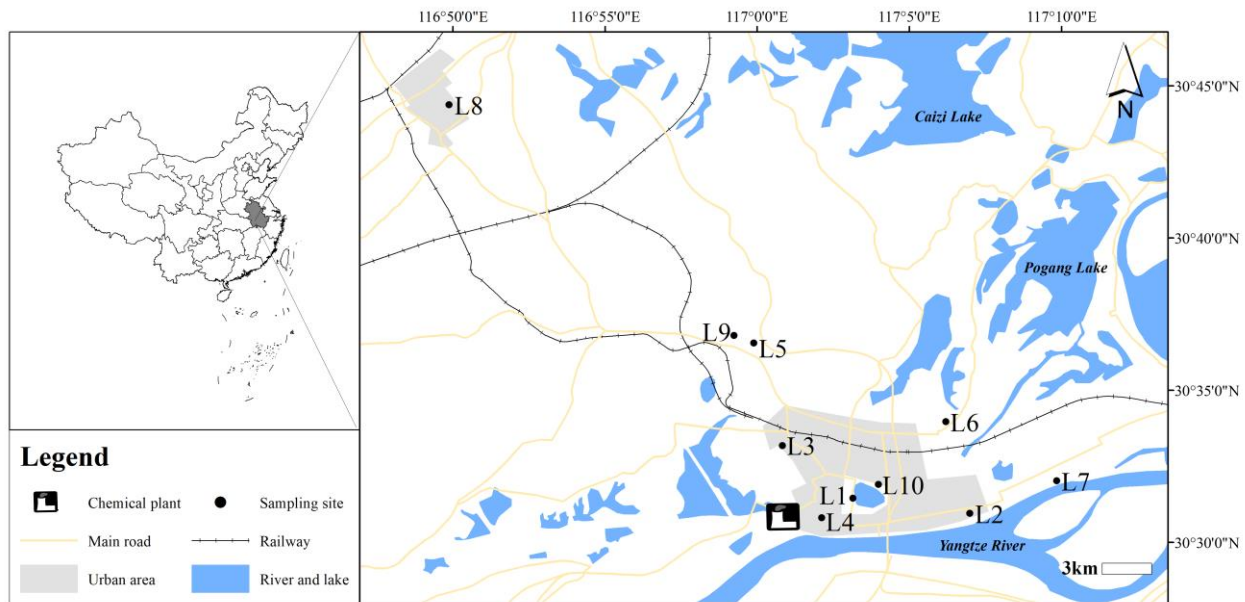
45 In recent years, people have gradually realised that PAHs contamination will constitute a great  
46 threat to public health, so the research on PAHs has become a hot spot. The research on PAHs in  
47 foreign countries started earlier, but the research on PAHs in China started later, and the cities that  
48 have carried out the research on PAHs in urban air are Shenzhen, Guangzhou, Tianjin, Xi'an and  
49 Beijing and other large cities(Fu et al., 2023, Jiang et al., 2023, Wu et al., 2022, Zhang et al., 2025,  
50 Li et al., 2022). Anqing, as a representative medium-sized industrial city in the Yangtze River  
51 Economic Belt, hosts a dense cluster of chemical, thermal power, steel, and building material  
52 industries(Sun et al., 2022). These sectors are characterized by intensive fossil fuel consumption and  
53 high-temperature processes, which are significant PAHs emission sources. Despite the proliferation  
54 of PAHs studies in megacities, systematic investigations in medium-sized industrial cities—  
55 particularly those with mixed industrial profiles like Anqing—remain scarce. This study aims to fill  
56 this gap by providing a comprehensive assessment of PAHs pollution characteristics, sources, and  
57 health risks in Anqing, thereby offering a scientific basis for targeted pollution control in similar  
58 urban contexts.

59 In this study, atmospheric dust deposition samples were collected from 10 different areas in  
60 Anqing City. The samples were extracted and concentrated using ultrasonic extraction before being  
61 quantitatively analysed for PAHs using gas chromatography-mass spectrometry (GC-MS). The  
62 primary objectives of this paper are to: (1) reveal the concentration and compositional characteristics  
63 of PAHs in atmospheric dust deposition in Anqing City; (2) identify the main origins of PAHs in  
64 atmospheric dust deposition; (3) assess the human health hazards associated with PAHs in  
65 atmospheric dust deposition.

## 66 **2. Materials and Methods**

### 67 2.1. Study area and sampling

68 In the last few years, the Anqing area of China has been designated a hub for chemical-based  
69 industries, boasting over 400 chemical companies, including Anqing Petrochemical and numerous  
70 others(Sun et al., 2022). With the concomitant increase in population and rapid economic growth, the  
71 issue of environmental pollution has become increasingly salient. In this study, 10 dust samples were  
72 gathered from diverse sites in Anqing City, with the sampling points distributed across the primary  
73 urban areas of Anqing City and Huaining County (Figure 1), covering industrial, commercial,  
74 residential, and suburban areas. During sampling, approximately 5 grams of dust is collected from  
75 outdoor window sills, etc., using a brush impregnated with acetone solution according to a strict  
76 procedure, and placed in a polythene sample bag labelled with the appropriate collection site.  
77 Subsequent to collection, the samples are returned to the laboratory to remove impurities, sieved  
78 through a 0.15 mm screen and stored at low temperatures.



80 **Figure 1.** Schematic diagram of atmospheric dust deposition sampling points

81 **2.2. Analysis of PAHs in atmospheric dust deposition**

82 The study analyzed the sixteen priority PAHs as identified by the USEPA, which include  
83 naphthalene (Nap), acenaphthylene (Acy), acenaphthene (Ace), fluoranthene (Fl), phenanthrene  
84 (Phe), anthracene (Ant), fluorene (Flu), pyrene (Py), benzo[a]anthracene (BaA), chrysene (Chry),  
85 benzo[a]pyrene (BaP), benzo[b]fluoranthene (BbF), benzo[k]fluoranthene (BkF), indeno[1,2,3-

86 cd]pyrene (InP), dibenzo[a,h]anthracene (DBA), and benzo[g,h,i]perylene (BghiP). Ultrasonic  
87 extraction method (USA EPA 3550B) was used. About 2 g of sediment was weighed, 2 g of copper  
88 powder was added, and the extract was extracted by ultrasonication with 15 mL of 1:1 (V:V) n-  
89 hexane/acetone solution for 30 min, centrifuged and transfer the supernatant, and the above  
90 ultrasonication was repeated for 2 times and the temperature was controlled to be below 40 °C. The  
91 extracts were combined, rotary evaporated to 2 mL, and the extracts were passed through a  
92 chromatography column (1 cm anhydrous sodium sulfate, 6 cm 3% deactivated alumina, and 12 cm  
93 3% deactivated silica gel from top to bottom). The column was pre-eluted with 15 mL of n-hexane,  
94 the hexane eluent was discarded, and then eluted with 70 mL of a (3:7 dichloromethane/n-hexane)  
95 mixture, all of which was received. The received solution was rotary evaporated and fixed to 1.0 mL  
96 with n-hexane, and stored at low temperature for measurement. The analysis of PAHs was conducted  
97 utilizing a GC-MS (Agilent 5975C/7890A) with ionization in electron impact (EI) mode, and data  
98 acquisition took place under the selective ion monitoring (SIM) mode.

### 99 2.3. Health risk assessment

100 The toxicity of PAHs present in atmospheric dust deposition is determined by means of the toxicity  
101 equivalency factor (TEF) of these compounds(Zhang et al., 2022). The most toxic PAH-BaP had a  
102 TEF value of 1, and the TEF values for the other PAHs were derived by comparing their  
103 carcinogenicity levels with those of BaP(Škrbić et al., 2019). CS denotes the total concentration of  
104 PAH congeners calculated using the TEF method (Equation (1))(Wang et al., 2011). Each PAH  
105 congener's concentration is denoted by  $C_n$  ( $m^3 \text{ kg}^{-1}$ ), and the corresponding TEF for each PAH is  
106 denoted by  $TEF_n$  (Table 2).

$$107 \quad CS = \sum (C_n \times TEF_n) \quad (1)$$

108 The incremental lifetime cancer risk (ILCR) associated with exposure to PAHs was determined  
109 based on previous research(Wu et al., 2020). The ILCRs for dermal contact, inhalation, and ingestion  
110 were quantified for each area dust sample in Anqing according to the following Equation (2) - (5):

111

$$\text{ILCR}_{\text{Ingestion}} = \frac{\text{CS} \times (\text{CSF}_{\text{Ingestion}} \times \sqrt[3]{\text{BW}/70}) \times \text{IR}_{\text{Ingestion}} \times \text{EF} \times \text{ED}}{\text{BW} \times \text{AT} \times 10^6} \quad (2)$$

112

$$\text{ILCR}_{\text{Inhalation}} = \frac{\text{CS} \times (\text{CSF}_{\text{Inhalation}} \times \sqrt[3]{\text{BW}/70}) \times \text{IR}_{\text{Inhalation}} \times \text{EF} \times \text{ED}}{\text{BW} \times \text{AT} \times \text{PEF}} \quad (3)$$

113

$$\text{ILCR}_{\text{Dermal}} = \frac{\text{CS} \times (\text{CSF}_{\text{Dermal}} \times \sqrt[3]{\text{BW}/70}) \times \text{SA} \times \text{AF} \times \text{ABS} \times \text{EF} \times \text{ED}}{\text{BW} \times \text{AT} \times 10^6} \quad (4)$$

114

$$\text{CR} = \text{ILCR}_{\text{Ingestion}} + \text{ILCR}_{\text{Inhalation}} + \text{ILCR}_{\text{Dermal}} \quad (5)$$

115 To minimise computational uncertainty, a Monte Carlo simulation (Oracle Crystal Ball, USA) was  
 116 employed. This simulation was based on parameters from previous researchs (Kong et al., 2025,  
 117 Tarafdar and Sinha, 2019)(Table 1) research and comprised 20,000 iterations.

Exposure variable	Distribution		Child	Unit
	types <sup>a</sup>	Adult		
Averaging life span (AT)	Point	70×365=25,550	70×365=25,550	day
Body weight (BW)	Normal	[52.10, 6.50]	[16.30, 2.40]	kg
Dermal exposure area (SA)	Lognormal	[4,619.11, 1.77]	[4,619.11, 1.77]	cm <sup>2</sup>
Dermal adherence factor (AF)	Lognormal	[0.04, 3.41]	[0.04, 3.41]	mg cm <sup>-2</sup>
Dermal adsorption fraction (ABS)	Lognormal	[0.13, 1.26]	[0.13, 1.26]	unitless
Exposure duration (ED)	Uniform	[0, 24]	[0, 6]	year
Exposure frequency (EF)	Triangular	345 [180, 365]	345 [180, 365]	day year <sup>-1</sup>
Ingestion rate (IR <sub>ingestion</sub> )	Point	100	200	mg day <sup>-1</sup>
Inhalation rate (IR <sub>inhalation</sub> )	Lognormal	[13.9, 1.07]	[7.19, 1.62]	m <sup>3</sup> day <sup>-1</sup>
Particle emission factor (PEF)	Point	1.36×10 <sup>9</sup>	1.36×10 <sup>9</sup>	m <sup>3</sup> kg <sup>-1</sup>
Ingestion carcinogenic slope factor (CSF <sub>ingestion</sub> )	Lognormal	[7.30, 1.15]	[7.30, 1.15]	mg kg <sup>-1</sup> day <sup>-1</sup>
Inhalation carcinogenic slope factor (CSF <sub>inhalation</sub> )	Lognormal	[3.14, 1.80]	[3.14, 1.80]	mg kg <sup>-1</sup> day <sup>-1</sup>
Dermal carcinogenic slope factor (CSF <sub>Dermal</sub> )	Point	25	25	mg kg <sup>-1</sup> day <sup>-1</sup>

119 <sup>a</sup> For normal, point, uniform and lognormal distributions, the values in parentheses represent the  
 120 arithmetic mean and standard deviation, the fixed values, the minimum and maximum, and the  
 121 geometric mean and geometric standard deviation, respectively.

122 2.4. Positive matrix factorization (PMF)

123 Source apportionment was performed using the US EPA PMF 5.0 model. The model decomposes  
124 the original data matrix  $X$  ( $n$  samples  $\times$   $m$  species) into factor contributions ( $G$ ) and factor profiles  
125 ( $F$ ), minimizing the objective function  $Q$ :

126 
$$X = G \times F + E \quad (6)$$

127 
$$Q = \sum_{i=1}^n \sum_{j=1}^m \left( \frac{e_{ij}}{u_{ij}} \right)^2 \quad (7)$$

128 where  $E$  is the residual matrix and  $u_{ij}$  is the uncertainty of species  $j$  in sample  $i$ .

129 Uncertainties ( $u_{ij}$ ) were calculated following (Guo et al., 2025b):

130 
$$u_{ij} = \begin{cases} 0.2 \times C_{ij} + \frac{MDL}{3}, & \text{if } C_{ij} \leq MDL \\ 0.1 \times C_{ij} + \frac{MDL}{3}, & \text{if } C_{ij} > MDL \end{cases} \quad (8)$$

131 where  $C_{ij}$  is the concentration and  $MDL$  is the method detection limit.

132 Model robustness was evaluated using multiple criteria. The optimal number of factors (three) was  
133 determined by examining the change in  $Q$  ( $Q_{\text{robust}}/Q_{\text{true}}$ ) with increasing factor numbers, ensuring  
134 physical interpretability of profiles. Bootstrap analysis (100 runs) was performed to assess factor  
135 stability and uncertainty. Key goodness-of-fit metrics, including the coefficient of determination ( $R^2$ )  
136 between observed and modeled concentrations for key species, are reported to validate model  
137 performance.

138 2.5. Quality assurance/quality control

139 To ensure the representativeness, accuracy, and comparability of the data, stringent quality control  
140 measures were implemented. Results for reagent blanks, laboratory blanks, and recovery experiments  
141 fell within acceptable ranges. Each PAH working standard curve exhibited good linearity with  
142 correlation coefficients ( $R^2$ )  $\geq 0.995$ . No PAHs were detected in reagent blanks. Laboratory blanks  
143 showed only trace amounts of Nap and Phe (below 3% of actual sample levels), with final  
144 concentrations adjusted by corresponding blank subtraction. The method's minimum detection limits  
145 ranged from 0.20 to 1.20 ng g<sup>-1</sup>. Except for the relatively low recovery rate of highly volatile

146 naphthalene (65.8%), recovery rates for other compounds ranged from 76 to 110%, with relative  
147 standard deviations < 8.0%. PAH concentrations in the measured dust were not corrected for recovery.

148 **3. Results and Discussion**

149 3.1. Distribution of PAHs content in dust

150 In this study, the contents of PAHs in dust samples from 10 sampling sites in urban areas of Anqing  
151 were counted. Table 2 lists the TEF, mean, median and range of 16 PAHs in the dust samples from  
152 the 10 sampling points.

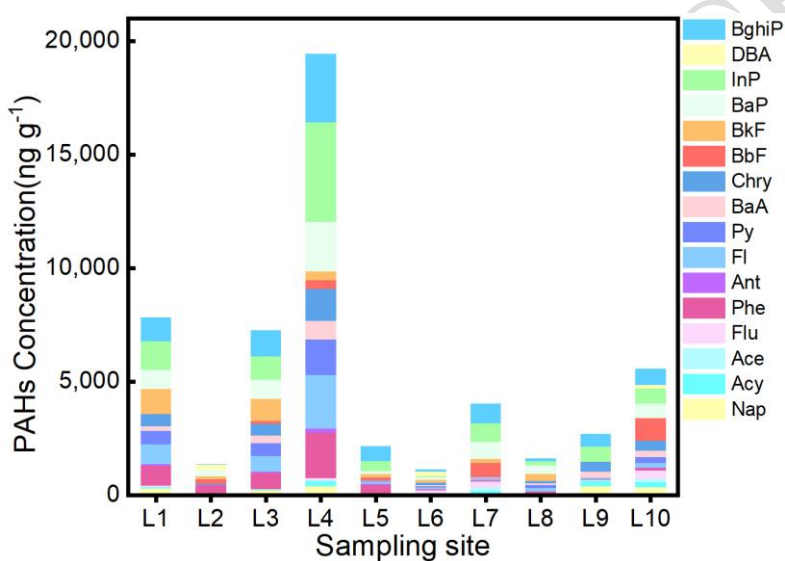
153 **Table 2.** Distribution of PAHs in dust samples from different areas of Anqing city.

Congeners	TEF	Mean(ng g <sup>-1</sup> )	Median(ng g <sup>-1</sup> )	Concentration(ng g <sup>-1</sup> )
Nap	0.001	175.016	127.96	0 - 409.51
Acy	0.001	98.229	42.12	0 - 232.7
Ace	0.001	46.33	19.475	0 - 157.06
Flu	0.001	93.833	28.16	0 - 365.27
Phe	0.001	482.271	273.635	17.11 – 2,005.35
Ant	0.01	38.783	14.335	1.75 - 194.64
F1	0.001	453.363	116.385	1.64 – 2,343.66
Py	0.001	323.667	80.505	0.96 – 1,567.34
BaA	0.1	211.601	138.275	15.57 - 815.77
Chry	0.01	365.861	266.145	28.29 – 1,408.7
BbF	0.1	245.095	122.935	0 - 998.03
BkF	0.1	334.646	170.54	0 – 1,077.93
BaP	1	616.714	525.87	0 – 2,177.43
InP	0.1	943.586	652.815	7.49 – 4,378.85
DBA	1	59.467	0	0 - 226.64
BghiP	0.01	812.849	679.085	12.41 – 2,992.15
$\sum_{16}^{} \text{PAHs}$	—	5,301.21	3,258.29	85.22 – 21,351.03

154 As shown in Table 2, the concentration of  $\sum_{16}^{} \text{PAHs}$  ranged from 85.22 - 21,351.03 ng g<sup>-1</sup>, with a  
 155 mean concentration of 5301.21 ng g<sup>-1</sup> and a median concentration of 3,258.29 ng g<sup>-1</sup>; of these, InP  
 156 had the highest concentration, with a mean concentration of 943.59 ng g<sup>-1</sup>, followed by BghiP and  
 157 BaP; Ant had the lowest concentration with an average of 38.79 ng g<sup>-1</sup>, while Ace and DBA also had  
 158 relatively low concentrations, detected in only 3 sampling sites. The minimum concentrations of the  
 159 2-ring PAHs (Nap, Acy, Ace, Flu) were all 0. This may be due to the fact that most of the 2-ring

160 PAHs are mainly present in the gas-phase and are volatile, and therefore their content in the particles  
161 may be below the detection limit.

162 Combined with Figure 2 we can clearly see the degree of contamination at each sampling point:  
163 L4>L1>L3>L10>L7>L9>L5>L8>L2>L6. It can be seen that the most serious pollution in the urban  
164 area of Anqing is Daguan District, Daguan District, there are Sinopec Anqing Petrochemical  
165 Company, Anqing Changhong Chemical Co., Ltd, Anqing Yicheng Chemical Technology Co., Ltd,  
166 Anqing Jingyi Fine Chemical Co., Ltd, and other chemical enterprises, and these chemical enterprises  
167 are very likely to be an important reason for the more serious pollution of PAHs in this area.



168

169 **Figure 2.** Distribution of PAHs in dust samples from different areas of Anqing city

170 Compared with other cities and countries, the levels of PAHs in atmospheric dust deposition in  
171 Anqing were significantly lower than those in Tianjin (average concentration of 7,990 ng g⁻¹)(Yu et  
172 al., 2014), Canada (average concentration of 24,700 ng g⁻¹)(Gill et al., 2020), Laiwu (average  
173 concentration of 10,892 ng g⁻¹)(Wei et al., 2021), and Shenzhen (average concentration of 29,920 ng  
174 g⁻¹)(Liu et al., 2016). The difference with Hubei Province (average concentration of 4,430 ng g⁻¹) is  
175 small(Zhang et al., 2016). It is not difficult to see that the average level of PAHs in atmospheric dust  
176 deposition in Anqing is lower than that in some large cities in China, which may be due to the high  
177 population density, motor vehicle emissions and fossil energy demand in large cities, and thus the

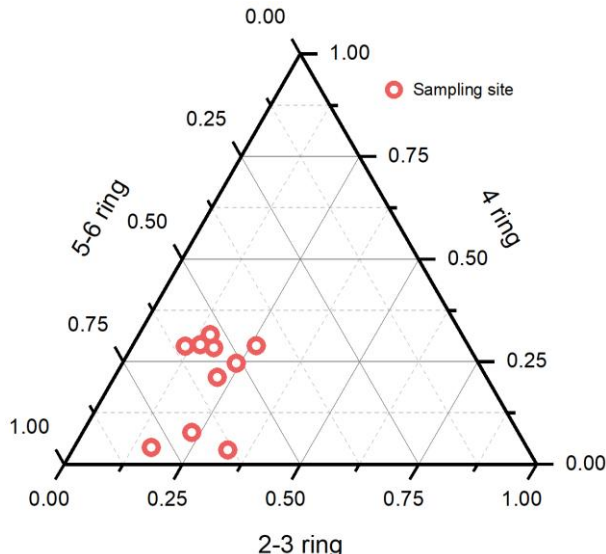
178 PAHs content in dust in large cities is much higher than that in small and medium-sized cities like  
179 Anqing.

180 Although this study's sample size is sufficient for a preliminary spatial assessment, it may limit the  
181 statistical robustness and spatial representativeness of the findings, particularly in heterogeneous  
182 urban environments. This limitation has been identified as a constraint of the study, and caution  
183 should be exercised when interpreting the results in relation to city-wide extrapolation. It should be  
184 noted that this study did not account for seasonal variations or meteorological influences, which may  
185 affect the deposition patterns and source contributions of PAHs. Future research should incorporate  
186 multi-seasonal sampling and atmospheric dispersion modelling to improve temporal  
187 representativeness.

188 3.2. Source analysis of PAHs in dust

189 3.2.1. Comparison of ring numbers of PAHs in dust

190 The distribution of PAHs with different ring numbers in the 10 dust samples collected in this  
191 experiment is shown in Figure 3, and the PAHs in the studied area are mainly 5-ring and 4-ring,  
192 followed by 3-ring. The other 16 PAHs can be divided into three groups according to their ring  
193 numbers: low molecular weight (2-3 ring, LMW), middle molecular weight (4 ring, MMW) and high  
194 molecular weight (5-6 rings, HMW) to discriminate their different sources of contamination. In  
195 general, LMW PAHs primarily originate from crude oil contamination and the combustion of  
196 materials such as wood and coal at temperatures below moderate levels(Zhang et al., 2020). MWM  
197 PAHs mainly stem from fuel combustion, while HWM PAHs primarily result from the high-  
198 temperature combustion of fossil fuels. The proportion of LMW PAHs in the dust samples in the  
199 studied area ranged from 11.30 - 32.95%, with a mean value of 20.32%, the proportion of MMW  
200 PAHs ranged from 3.43 - 31.59%, with a mean value of 20.78%, and the proportion of HMW PAHs  
201 ranged from 44.83 - 79.42%, with a mean value of 58.90%. This indicates that PAHs in atmospheric  
202 dust deposition in Anqing City primarily originate from high-temperature combustion processes, such  
203 as coal combustion and motor vehicle exhaust emissions.

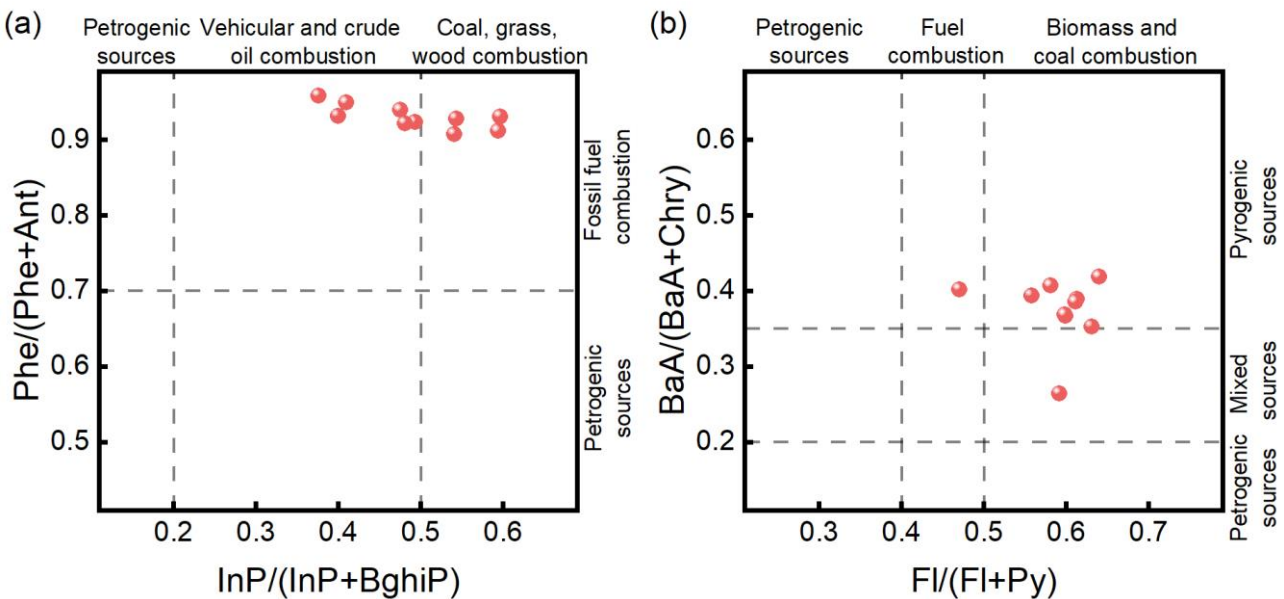


204

205 **Figure 3.** Ternary plot showing comparative contribution of 2–3 ring, 4 ring and 5–6 ring PAHs in  
206 samples

207 3.2.2. Characteristic ratio method of PAHs in dust

208 In order to gain a more detailed understanding of the emission origins of PAHs in atmospheric  
209 dust deposition, a diagnostic comparison of PAHs was performed, the results of which are shown in  
210 Figure 4(Li et al., 2017). The majority of the samples exhibited  $F1/(F1 + Py)$  ratios greater than 0.5,  
211 suggesting a mixture of fuel combustion sources(Han et al., 2021). The ratios of  $BaA/(BaA + Chry)$   
212 and  $InP/(InP + BghiP)$  both exceeded 0.2, indicating that the primary origins of PAHs in atmospheric  
213 dust deposition were emissions from coal, wood, fuel combustion, and vehicular exhaust(Wang et al.,  
214 2022). The predominance of PAHs at most road atmospheric samples, as indicated by ratios of  
215  $Phe/(Phe + Ant) > 0.7$ , was attributed to fossil fuel combustion(Zhang et al., 2024).



216 **Figure 4.** Characteristic ratios of PAHs in dust in different areas of Anqing City

217 In summary, the PAHs in atmospheric dust deposition in Anqing City primarily originate from a  
 218 combination of pollution sources, including fossil fuel combustion, coal combustion, and motor  
 219 vehicle emissions. The pollution source structure was similar across all sampling sites, with no  
 220 significant spatial variation observed.

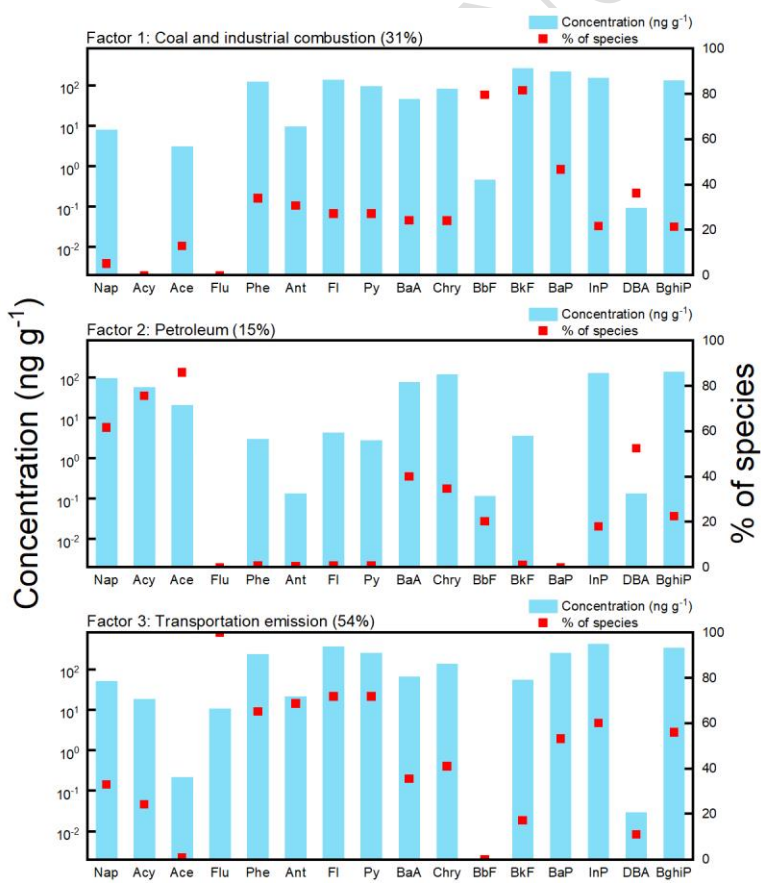
221 3.2.3. PMF of PAHs in dust

222 To identify the primary sources of PAHs in atmospheric dust deposition, this study employed a  
 223 positive matrix factorization model for source apportionment of 16 PAHs. Based on model goodness-  
 224 of-fit and factor independence, three factors were ultimately determined as the optimal solution. The  
 225 loadings of PAHs across each factor and their contributions to total concentration are shown in Figure  
 226 5.

227 Factor 1 explained 30.66% of the total PAH concentration, primarily contributed by high-  
 228 molecular-weight PAHs such as BkF (81.65%), BaP (46.77%), and InP (21.77%). These compounds  
 229 are typically associated with high-temperature combustion processes, particularly coal combustion  
 230 and industrial high-temperature operations(Wang et al., 2025). Additionally, medium-ring PAHs like  
 231 Phe, Fla, and Pyr constitute a significant proportion within this factor, further supporting its  
 232 combustion-derived characteristics. Thus, factor 1 is identified as originating from coal and industrial  
 233 combustion sources.

235 Factor 2 contributed 15.49% of the total concentration, primarily loaded onto low-ring PAHs such  
236 as Acy (75.75%), Ace (86.07%), and BaA (40.11%). These compounds are frequently associated with  
237 incomplete combustion of biomass or volatilization of petroleum substances(Guo et al., 2025a).  
238 Notably, Acy and Ace are widely recognized as tracers of biomass combustion. Therefore, factor 2 is  
239 classified as a biomass and petroleum volatiles source.

240 Factor 3 is the largest contributing source, accounting for 53.85% of total PAH concentration. It  
241 primarily includes medium-to-low ring PAHs such as Flu (100%), Phe (65.20%), Fl (71.84%), and  
242 Py (71.94%). These compounds are commonly found in transportation emissions, particularly  
243 gasoline vehicle exhaust(Ma et al., 2025). Additionally, InP and BghiP constitute a significant  
244 proportion within this factor, further supporting its association with motor vehicle emissions.  
245 Consequently, factor 3 is identified as a transportation emission source.



246

247

248 The contribution order of the three sources to total PAHs was: traffic emissions (53.85%) > coal  
249 and industrial combustion (30.66%) > biomass and petroleum volatiles (15.49%). Coal and industrial

**Figure 5.** Analysis of sources of PAHs based on PMF

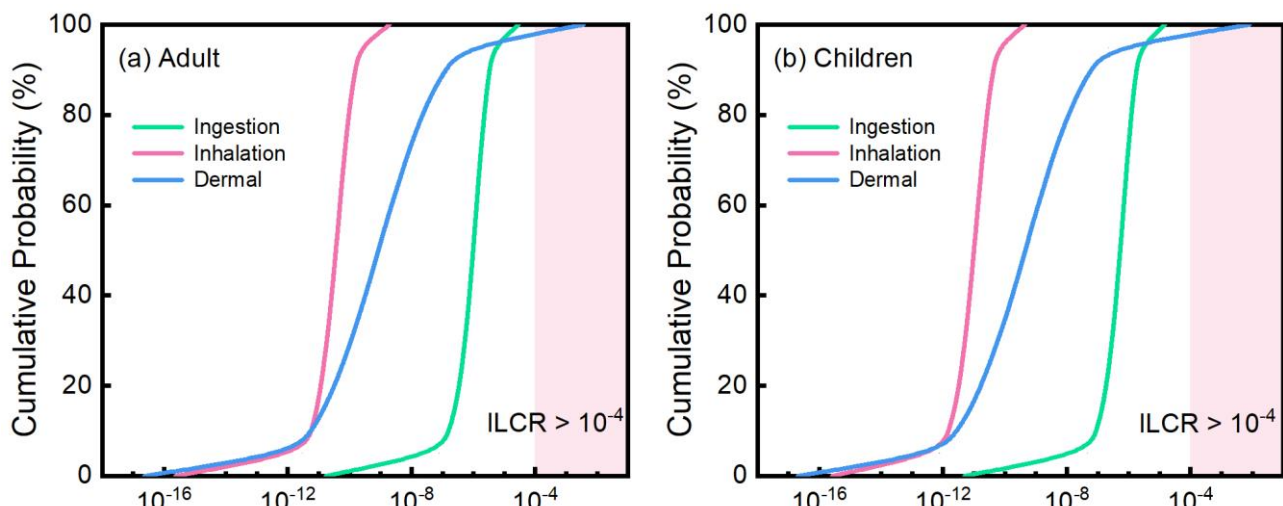
250 combustion contributed more than in Shanghai (14.7 %)(Feng et al., 2022) but less than in Anshan  
251 (32.6 %)(Wang et al., 2020). This source profile aligns with Anqing's status as an industrial city with  
252 growing vehicular activity. Comparing with other Chinese cities, the contribution of traffic sources  
253 here (53.85%) is higher than in some heavily industrial cities where coal combustion dominates,  
254 highlighting the need for targeted vehicular emission controls alongside industrial regulations.

255 3.3. Health risk assessment of PAHs

256 This study employed Monte Carlo simulations to assess the ILCR of PAHs in atmospheric dust  
257 deposition for adults and children(Bharali et al., 2025). Overall, dermal contact and oral ingestion  
258 represent the predominant exposure pathways, while inhalation risks are negligible.

259 As shown in the ILCR probability distribution in Figure 6, both adults and children exhibit  
260 significantly right-skewed risk distributions for skin contact and oral ingestion, with pronounced  
261 high-risk “tails.” Notably, in the skin contact pathway, the rightmost tail of the distribution curve  
262 approaches or even exceeds  $1\times10^{-4}$ , indicating that skin contact may pose unacceptable carcinogenic  
263 risks under extreme exposure scenarios(Sun et al., 2025).

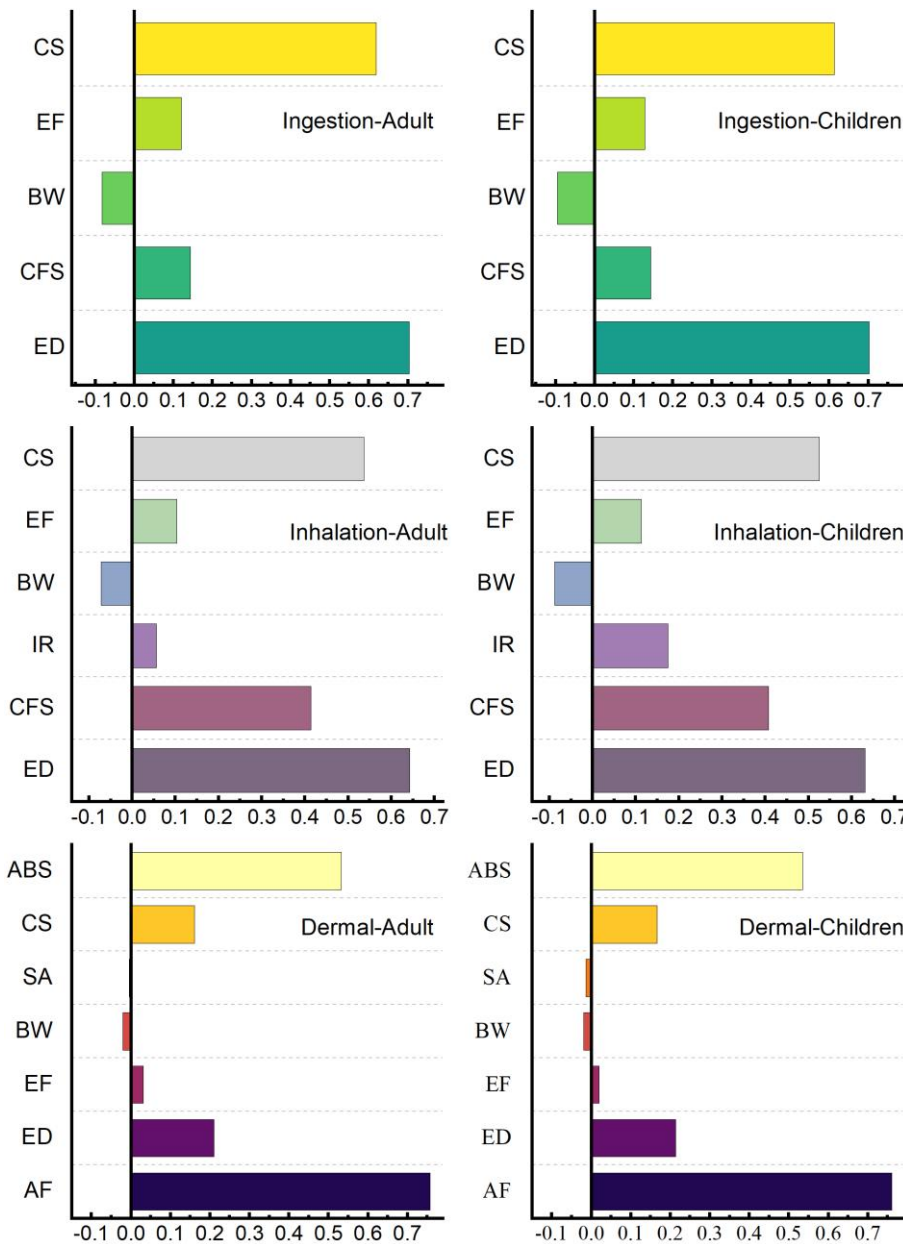
264 Although the median and mean ILCR values for skin contact are below  $10^{-4}$ , the high-end quantiles  
265 (e.g., 95th percentile or higher) suggest that for a portion of highly exposed individuals  
266 (approximately 5% or less), the carcinogenic risk via this route may have reached levels warranting  
267 intervention. This finding aligns with the high contribution of the AF in sensitivity analyses,  
268 indicating that individual behavioral variations and uncertainties in exposure levels are key drivers of  
269 the high-risk tail.



271 **Figure 6.** Probability distribution for carcinogenic risks of PAHs for (a) adults and (b) children

272 As shown in Figure 7, ED and BaP equivalent toxicity concentration (CS) are the most sensitive  
 273 parameters across all exposure pathways. For the dermal exposure pathway, the AF is also a critical  
 274 influencing factor(Khalili et al., 2021). This indicates that, in addition to controlling the toxic  
 275 equivalent concentration of dust, reducing the frequency of skin contact with dust and the amount of  
 276 dust adhering to the skin—particularly through protective measures in high-risk environments such  
 277 as frequent ground activities and cleaning operations—is especially crucial for controlling the high  
 278 tail risk associated with the dermal pathway.

279 In summary, although the average carcinogenic risk from PAHs in indoor dust is generally  
 280 manageable, skin contact exposure under extreme conditions may pose unacceptable health risks  
 281 ( $ILCR > 10^{-4}$ ). This finding underscores that risk assessment and management should prioritize high-  
 282 risk populations and extreme exposure scenarios, beyond merely monitoring average risk levels. This  
 283 underscores that, in addition to reducing environmental PAHs concentrations, behavioral and  
 284 exposure mitigation measures—such as improved hygiene practices, use of protective gear for  
 285 outdoor workers, and reducing children's direct contact with dust—are crucial for managing  
 286 population risk, especially for vulnerable subgroups.



287  
288 **Figure 7.** Sensitivity analysis of ILCR for PAHs

289 **4. Conclusions**

290 This study systematically examined the pollution levels, composition profiles, sources, and health  
291 risks of 16 priority PAHs in atmospheric dust deposition across different functional zones in Anqing  
292 City, China. The concentration range of  $\Sigma_{16}$ PAHs in atmospheric dust in Anqing City was relatively  
293 wide (85.22 – 21,351.03 ng g<sup>-1</sup>), with an average concentration of 5,301.21 ng g<sup>-1</sup>, indicating a  
294 pollution level in the lower-middle range nationally. Spatial distribution revealed significantly higher  
295 concentrations in industrial clusters like Daguan District (L1, L3, L4) compared to other areas,  
296 indicating local industrial emissions as a major point source of PAHs. Composition analysis showed

297 high-ring (5–6 ring) PAHs dominated (average 58.90%), revealing that PAHs in the study area  
298 primarily originate from high-temperature combustion processes. Comprehensive source  
299 apportionment using ring number distribution, characteristic ratio method, and PMF models yielded  
300 mutually corroborating results, confirming that Anqing's PAH pollution stems from a hybrid  
301 contamination pattern involving fossil fuel combustion and industrial activities. Probabilistic health  
302 risk assessment was conducted using a Monte Carlo simulation-based ILCR model. Results indicate  
303 that for the general population of Anqing City, the overall carcinogenic risk from PAH exposure via  
304 particulate matter deposition is at an acceptable level. Skin contact is the primary exposure pathway,  
305 with its high-risk tail (e.g., 95th percentile) approaching or reaching  $10^{-4}$ , warranting attention.  
306 Children's total risk is slightly higher than adults', which is associated with their behavioral patterns  
307 (frequent hand-to-mouth contact).

## 308 **5. Environmental implications**

309 The findings underscore that in industrial cities like Anqing, control strategies must adopt a multi-  
310 target approach. Prioritizing traffic emission reductions (e.g., upgrading vehicle fleets, promoting  
311 EVs) is essential, given its dominant contribution. Simultaneously, stringent controls on industrial  
312 and coal combustion emissions are needed, especially in identified hotspot areas like Daguan District.  
313 Public health measures should focus on reducing dermal exposure for high-risk groups (children,  
314 outdoor workers). This study establishes a critical baseline and a methodological framework  
315 (integrating PMF and probabilistic risk assessment) that can be applied to other industrial cities for  
316 evidence-based environmental management.

## 317 **Acknowledgements**

318 This research project was supported financially through the Scientific Research Project of Higher  
319 Education Institutions in Anhui Province (Natural Sciences: grant number 2023AH040070).

## 320 **Conflict of Interest**

321 The authors declare no conflict of interest.

## 322 **References**

- 323 Barbosa Jr, F., Rocha, B. A., Souza, M. C. O., Bocato, M. Z., Azevedo, L. F., Adeyemi, J. A., Santana,  
324 A. & Campiglia, A. D. 2023. Polycyclic aromatic hydrocarbons (PAHs): Updated aspects of  
325 their determination, kinetics in the human body, and toxicity. *Journal of Toxicology and*  
326 *Environmental Health, Part B*, **26**, 28–65.
- 327 Bharali, P., Gupta, N., Agarwal, T., Balachandran, S. & Hoque, R. R. 2025. Polycyclic Aromatic  
328 Hydrocarbons (PAHs) in park and playground soils: A comparative health risk assessment in  
329 two South Asian cities of Brahmaputra Valley, India. *Environmental Pollution*, **382**, 126699.
- 330 Feng, X., Feng, Y., Chen, Y., Cai, J., Li, Q. & Chen, J. 2022. Source apportionment of PM2.5 during  
331 haze episodes in Shanghai by the PMF model with PAHs. *Journal of Cleaner Production*,  
332 **330**, 129850.
- 333 Fu, J., Ji, J., Luo, L., Li, X., Zhuang, X., Ma, Y., Wen, Q., Zhu, Y., Ma, J., Huang, J., Zhang, D. &  
334 Lu, S. 2023. Temporal and spatial distributions, source identification, and health risk  
335 assessment of polycyclic aromatic hydrocarbons in PM2.5 from 2016 to 2021 in Shenzhen,  
336 China. *Environmental Science and Pollution Research*.
- 337 Gill, R., Hurley, S., Brown, R., Tarrant, D., Dhaliwal, J., Sarala, R., Park, J.-S., Patton, S. & Petreas,  
338 M. 2020. Polybrominated Diphenyl Ether and Organophosphate Flame Retardants in  
339 Canadian Fire Station Dust. *Chemosphere*, **253**, 126669.
- 340 Guo, J., Xie, Y., Dou, X., Qi, W., Liao, Y., Cao, X., Peng, J. & Liu, H. 2025a. Combining source  
341 identification and risk assessment to uncover spatial risk patterns in an agricultural lake.  
342 *Journal of Environmental Management*, **387**, 125966.
- 343 Guo, Z., Sun, S., Cao, R., Jiang, N., Liang, N., Wang, Z., Guo, J., Li, M., Liu, X., Geng, N. & Chen,  
344 J. 2025b. Tracing toxic pollutants in coastal urban atmosphere: A case study on the particle-  
345 size distribution, sources, and health risks of PCDD/Fs, PCBs, PAHs, and substituted PAHs.  
346 *Journal of Hazardous Materials*, **498**, 139833.
- 347 Han, L., Liu, Y., Hong, J., Wang, F., Song, N. & Su, B. 2021. DISTRIBUTION, SOURCE  
348 IDENTIFICATION AND RISK ASSESSMENT OF POLYCYCLIC AROMATIC

- 349 HYDROCARBONS IN ARABLE SOILS AT A TYPICAL LONG TERM COKING  
350 PRODUCTION BASE IN NORTH CHINA. *Fresenius Environmental Bulletin*, **30**, 697–706.
- 351 Jiang, G., Song, X., Xie, J., Shi, T. & Yang, Q. 2023. Polycyclic aromatic hydrocarbons (PAHs) in  
352 ambient air of Guangzhou city: Exposure levels, health effects and cytotoxicity.  
353 *Ecotoxicology and Environmental Safety*, **262**.
- 354 Khalili, F., Shariatifar, N., Dehghani, M. H., Yaghmaeian, K., Nodehi, R. N. & Yaseri, M. 2021. The  
355 analysis and probabilistic health risk assessment of PAHs in vegetables and fruits samples  
356 marketed Tehran Chemometric. *Global NEST Journal*, **23**, 497–508.
- 357 Kong, J., Yan, S., Cao, X., Zhang, Y., Ran, C., Chen, X., Yang, S., Li, S., Zhang, L. & He, H. 2025.  
358 Quantitative source apportionment and health risk assessment for polycyclic aromatic  
359 hydrocarbon and their derivatives in indoor dust from housing and public buildings of a mega-  
360 city in China. *Journal of Hazardous Materials*, **486**, 137057.
- 361 Kothiyal, N. C., Abhay, Khan, L., Kumar, Saruchi & Singh, S. 2022. Recent advances in emission,  
362 analysis and remediation technique of carcinogenic polycyclic aromatic hydrocarbons: a  
363 review. *Global NEST Journal*, **24**, 177–194.
- 364 Li, Y., Bai, X., Ren, Y., Gao, R., Ji, Y., Wang, Y. & Li, H. 2022. PAHs and nitro-PAHs in urban  
365 Beijing from 2017 to 2018: Characteristics, sources, transformation mechanism and risk  
366 assessment. *Journal of Hazardous Materials*, **436**.
- 367 Li, Y., Song, N., Yu, Y., Yang, Z. & Shen, Z. 2017. Characteristics of PAHs in street dust of Beijing  
368 and the annual wash-off load using an improved load calculation method. *Science of The Total  
369 Environment*, **581-582**, 328–336.
- 370 Liu, L., Liu, A., Li, Y., Zhang, L., Zhang, G. & Guan, Y. 2016. Polycyclic aromatic hydrocarbons  
371 associated with road deposited solid and their ecological risk: Implications for road  
372 stormwater reuse. *Science of The Total Environment*, **563-564**, 190–198.

- 373 Ma, X., Huang, C., Li, Y., Li, S., Jiang, Q., Zhang, C., Xue, B. & Yang, H. 2025. Influencing factors  
374 and risk assessment of polycyclic aromatic hydrocarbons in the sediments of Beilianchi Lake,  
375 China. *Science of The Total Environment*, **981**, 179607.
- 376 Ma, Y., Liu, A., Egodawatta, P., McGree, J. & Goonetilleke, A. 2017. Quantitative assessment of  
377 human health risk posed by polycyclic aromatic hydrocarbons in urban road dust. *Science of  
378 The Total Environment*, **575**, 895–904.
- 379 Samburova, V., Zielinska, B. & Khlystov, A. 2017. Do 16 Polycyclic Aromatic Hydrocarbons  
380 Represent PAH Air Toxicity? *Toxics*, **5**, 17.
- 381 Škrbić, B., Đurišić-Mladenović, N., Živančev, J. & Tadić, Đ. 2019. Seasonal occurrence and cancer  
382 risk assessment of polycyclic aromatic hydrocarbons in street dust from the Novi Sad city,  
383 Serbia. *Science of The Total Environment*, **647**, 191–203.
- 384 Sun, J., Zhao, M., Huang, J., Liu, Y., Wu, Y., Cai, B., Han, Z., Huang, H. & Fan, Z. 2022.  
385 Determination of priority control factors for the management of soil trace metal(loid)s based  
386 on source-oriented health risk assessment. *Journal of Hazardous Materials*, **423**, 127116.
- 387 Sun, Y., Miao, J., Huang, R., Tang, W., Wang, S., Li, P., Qian, W., Lee, J.-S., Wang, T. & Zhu, X.  
388 2025. Occurrence, distribution, and ecological risks of organic pollutants in global mangrove  
389 sediments. *Journal of Hazardous Materials*, **499**, 140032.
- 390 Tarafdar, A. & Sinha, A. 2019. Health risk assessment and source study of PAHs from roadside soil  
391 dust of a heavy mining area in India. *Archives of Environmental & Occupational Health*, **74**,  
392 252–262.
- 393 Wang, H., Chen, Z., Walker, T., Wang, Y., Luo, Q., Wu, H. & Wang, X. 2022. Characterization,  
394 source apportionment and risk assessment of PAHs in urban surface dust in Shenyang city,  
395 China. *Environmental Geochemistry and Health*, **44**, 3639–3654.
- 396 Wang, S., Ji, Y., Zhao, J., Lin, Y. & Lin, Z. 2020. Source apportionment and toxicity assessment of  
397 PM2.5-bound PAHs in a typical iron-steel industry city in northeast China by PMF-ILCR.  
398 *Science of The Total Environment*, **713**, 136428.

- 399 Wang, W., Huang, M.-j., Kang, Y., Wang, H.-s., Leung, A. O. W., Cheung, K. C. & Wong, M. H.  
400 2011. Polycyclic aromatic hydrocarbons (PAHs) in urban surface dust of Guangzhou, China:  
401 Status, sources and human health risk assessment. *Science of The Total Environment*, **409**,  
402 4519–4527.
- 403 Wang, X., Zhao, S., Tang, J., Yao, C., Tian, L., Tian, C., Ma, W., Zhang, G. & Li, J. 2025. Decadal  
404 Shifts in PAH Sources and Health Risks in China under Clean Air Actions. *Environmental*  
405 *Science & Technology*.
- 406 Wei, X., Ding, C., Chen, C., Zhu, L., Zhang, G. & Sun, Y. 2021. Environment impact and  
407 probabilistic health risks of PAHs in dusts surrounding an iron and steel enterprise. *Scientific*  
408 *Reports*, **11**, 6749.
- 409 Wu, Y., Zhang, N., Wang, Y., Ren, Y., Yuan, Z. & Li, N. 2020. Concentrations of polycyclic aromatic  
410 hydrocarbons in street dust from bus stops in Qingyang city: Estimates of lifetime cancer risk  
411 and sources of exposure for daily commuters in Northwest China. *Environmental Pollution*,  
412 **266**, 115222.
- 413 Wu, Z., He, C., Lyu, H., Ma, X., Dou, X., Man, Q., Ren, G., Liu, Y. & Zhang, Y. 2022. Polycyclic  
414 aromatic hydrocarbons and polybrominated diphenyl ethers in urban road dust from Tianjin,  
415 China: pollution characteristics, sources and health risk assessment. *Sustainable Cities and*  
416 *Society*, **81**.
- 417 Yang, L., Zhang, H., Zhang, X., Xing, W., Wang, Y., Bai, P., Zhang, L., Hayakawa, K., Toriba, A.  
418 & Tang, N. 2021. Exposure to Atmospheric Particulate Matter-Bound Polycyclic Aromatic  
419 Hydrocarbons and Their Health Effects: A Review. *International Journal of Environmental*  
420 *Research and Public Health*, **18**.
- 421 Yu, B., Xie, X., Ma, L. Q., Kan, H. & Zhou, Q. 2014. Source, distribution, and health risk assessment  
422 of polycyclic aromatic hydrocarbons in urban street dust from Tianjin, China. *Environmental*  
423 *Science and Pollution Research*, **21**, 2817–2825.

- 424 Zhang, J., Liu, F., Huang, H., Wang, R. & Xu, B. 2020. Occurrence, risk and influencing factors of  
425 polycyclic aromatic hydrocarbons in surface soils from a large-scale coal mine, Huainan,  
426 China. *Ecotoxicology and Environmental Safety*, **192**, 110269.
- 427 Zhang, J., Zhan, C., Liu, H., Liu, T., Yao, R., Hu, T., Xiao, W., Xing, X., Xu, H. & Cao, J. 2016.  
428 Characterization of Polycyclic Aromatic Hydrocarbons (PAHs), Iron and Black Carbon  
429 within Street Dust from a Steel Industrial City, Central China. *Aerosol and Air Quality  
430 Research*, **16**, 2452–2461.
- 431 Zhang, P., Zhao, Y., Yang, B., Wang, X., Qin, G., Zhao, G., Wang, T., Sun, P. & Zhang, Y. 2025.  
432 Pollution characteristics, source analysis, and health risk assessment of polycyclic aromatic  
433 hydrocarbons in atmospheric PM2.5: a case study in Xi'an, China. *International Journal of  
434 Environmental Health Research*.
- 435 Zhang, X., Wang, X., Zhao, X., Tang, Z., Zhao, T., Teng, M., Liang, W., Wang, J. & Niu, L. 2022.  
436 Using deterministic and probabilistic approaches to assess the human health risk assessment  
437 of 7 polycyclic aromatic hydrocarbons. *Journal of Cleaner Production*, **331**.
- 438 Zhang, X., Yao, Z., Yang, W., Zhang, W., Liu, Y., Wang, Z. & Li, W. 2024. Distribution, sources,  
439 partition behavior and risk assessment of polycyclic aromatic hydrocarbons (PAHs) in the  
440 waters and sediments of Lake Ulansuhai, China. *Marine Pollution Bulletin*, **200**.

441